

Evaluation of the Influence of the Substituting Cation on the Structural and Morphological Properties of the New Garnet $\text{Sm}_{3-x}\text{REE}_x\text{Fe}_5\text{O}_{12}$ (REE = Dy, Gd and Lu)

Angela Maria Morales Rivera^{a,b,*}, Luis Carlos Moreno Aldana^a, Carlos Arturo Parra Vargas^b

^aLaboratorio de Catálisis Heterogénea, Universidad Nacional de Colombia, Carrera 45 No 26-85, Bogotá, Colombia

^bGrupo de Física de Materiales, Universidad Pedagógica y Tecnológica de Colombia, Avenida Central del Norte 39-115 Tunja, Boyacá, Colombia

Received: May 07, 2019; Revised: September 12, 2019; Accepted: November 14, 2019

Rare earth garnets ($\text{REE}_3\text{Fe}_5\text{O}_{12}$) have magnetic-electric and optical properties that can be used in transmitters, microwave and data storage devices. These properties depend mainly on partial or total substitution of the cationic sites, as well as by the synthesis method used. Therefore, in this work was studied the influence of the substituting cation on the structural and morphological properties of new garnets with formula $\text{Sm}_{3-x}\text{REE}_x\text{Fe}_5\text{O}_{12}$ with $x = 0.0 - 1.0$; obtained by the solid-state reaction method. Characterization of samples was carried out by XRD, Rietveld refinement, SEM and Raman spectroscopy. The results showed that the substitution favors system stability and formation of garnets single phase with cubic structure and space group of $Ia\bar{3}d$ (230) at temperatures lower than reported by other authors. The substitution generated a decrease of the lattice parameters, the crystal size and favored particle formation of the order of micrometers (from 1.3 to 3.6 μm).

Keywords: Rare earth garnets, solid state reaction.

1. Introduction

The iron-rare earth garnets $\text{REE}_3[\text{Fe}_2](\text{Fe}_3)\text{O}_{12}$ crystallize in the cubic system and present space group $Ia\bar{3}d$ (230), the unit cell is constituted by three crystallographic sites: tetrahedral site 24d (Fe_2), octahedral site 16a [Fe_3] and dodecahedral site 24c REE_3 ¹. Thanks to this structural distribution, garnets can be constituted by different ions that give them remarkable magnetic-electric and optical properties².

Yttrium-iron garnet ($\text{Y}_3\text{Fe}_5\text{O}_{12}$) is the most important material in this family of oxides: it is ferrimagnetic with high Curie temperature ($T_c = 260$ °C), it has low coercive field (H_c) and high thermal conductivity, electrical resistivity and Verdet constant, which results in the Faraday effect or magneto-optic effect³. Thanks to these properties, further investigations studied the effect of yttrium substitution by rare earth elements (REE) such as neodymium (Nd), samarium (Sm), gadolinium (Gd), holmium (Ho) and dysprosium (Dy) and cerium (Ce)⁴; this allowed to discover the existence of magnetic anisotropy, magneto-dielectric, magneto-electric and magneto optical effects associated with these new materials^{5,6}.

The magneto-optical and electrical properties depend on the composition, structure and morphology of the material, which are mainly influenced by the cation or substituent cations and the synthesis method, allowing its application in microwave devices, optical oscillators, phase shifters, radars and for data storages devices⁷. The synthesis methods mainly used to obtain garnets are: the solid-state reaction method and the sol-gel method. Deka *et al.* synthesized the $\text{Y}_{3-x}\text{Sm}_x\text{Fe}_5\text{O}_{12}$ system with $x = 0.0$ to 3.0 of pure phase by the solid-state reaction method with synthesis temperatures of 1400 °C in the year 2017⁸.

Also, in 2017 they reported the synthesis of $\text{Sm}_3\text{Fe}_5\text{O}_{12}$ with a calcination temperature of 1200 °C and a sintering temperature of 1400 °C⁹. In the same year Jang *et al.* reported the synthesis of $\text{Y}_3\text{Fe}_5\text{O}_{12}$ obtained by the sol-gel method with a temperature of 1400 °C¹⁰; similarly, Tholkappiyan *et al.* reported the same sintering temperature for dysprosium iron garnet ($\text{Dy}_3\text{Fe}_5\text{O}_{12}$), showing the formation of thick and pure phase microstructures¹¹.

The applications will not only be modified by the synthesis method used, but also by the cation that replaces the dodecahedral site of the structure, as reported by Ramesh *et al.* who demonstrated that the substitution of $\text{Y}_3\text{Fe}_5\text{O}_{12}$ by gadolinium allows applications in optical isolators and communication systems¹². Substitution with Gd improves the magnetic properties and microwave absorption, allowing its application in microwave devices and magneto-optical insulators^{13,14}. The substitution with Dy modifies the dielectric and magnetic properties, making it a promising material for use in radars, television screens fabrication and data storage due to the great of Faraday rotation ($1 \times 10^5 \text{ cm}^{-1}$)¹⁵. Finally, it has been established that the insertion of lutetium (Lu) does not contribute to any magnetic behavior due to the absence of unpaired electrons ($4f^4$), therefore, the net magnetic moment will be given by the unequal distribution of the octahedral and tetrahedral Fe^{3+} ions. It presents important applications in telecommunications and data storage industry due to this magnetic-dielectric coupling¹⁶.

In this work, new garnets with formula $\text{Sm}_{3-x}\text{REE}_x\text{Fe}_5\text{O}_{12}$ (REE = Dy, Gd and Lu) were synthesized and characterized with seven different substitution values ($x = 0.0, 0.1, 0.2, 0.4, 0.6, 0.8$ and 1.0) by the solid state reaction method.

*e-mail: ammoralessri@unal.edu.co

The phase, the crystalline structure and the surface morphology were studied using XRD, SEM and Raman; this procedure allowed evaluating the influence the substituting cation has on the garnet's structural and morphological properties.

2. Experimental

2.1 Synthesis of samples

The garnets $\text{Sm}_{3-x}\text{REE}_x\text{Fe}_5\text{O}_{12}$ (REE = Dy, Gd and Lu) with $x = 0.0, 0.1, 0.2, 0.4, 0.6, 0.8$ and 1.0 were synthesized by the solid-state reaction method, from stoichiometric amounts of oxides: Sm_2O_3 (99.99% Sigma Aldrich), Dy_2O_3 (99.999% Sigma Aldrich), Gd_2O_3 (99.999% Sigma Aldrich), Lu_2O_3 (99.99% Sigma Aldrich) and Fe_2O_3 (99.99% Sigma Aldrich) previously calcined at 800°C for 2 h in order to eliminate carbon compounds and water present superficially.

Each mixture with stoichiometric amounts of oxides was subjected to grinding processes, and calcination at 800°C to obtain a mixture as homogeneous as possible. Then it was ground, pressed into pellets at pressure of 2.5 MPa and subjected to a sintering process at 1200°C for 20 h in order to favor the interdiffusion processes that allowed the obtention of the desired crystalline phase.

2.2 Characterization of samples

The mixed oxides obtained in pellet, were characterized through X-ray diffraction (XRD), in a PANalytical X Pert PRO-MPD equipment with Bragg-Brentano configuration, using the $\text{CuK}\alpha$ radiation ($\lambda = 1.5406 \text{ \AA}$) 15° and $90^\circ 2\theta$. The Rietveld refinement was made using the GSAS and PCW softwares. The morphological properties of the solids were evaluated by scanning electron microscopy (SEM) in a Tescan Vega 3 SB, the analysis of the micrographs was done using the Image J program and finally the analysis by Raman spectroscopy was made an DRX Raman Microscope- Thermo Scientific equipment with a laser of 532 nm .

3. Results and Discussion

3.1 Structural analysis

Figs. 1 to 3 show the X-ray diffraction patterns taken in pellets of each of the garnet-type $\text{Sm}_{3-x}\text{REE}_x\text{Fe}_5\text{O}_{12}$ (REE = Gd, Dy and Lu) with $x = 0.0, 0.1, 0.2, 0.4, 0.6, 0.8$ and 1.0 synthesized by the solid state reaction method at a temperature of 1200°C . The analysis allowed to determine a phase classification according to the iron-samarium garnet with reference code JCPDS 01-073-1379, of cubic structure, space group $Ia\bar{3}d$ (230) and with a preferential orientation in along (4 2 0) crystal plane, which corresponds to peak with higher intensity in the theoretical XRD pattern.

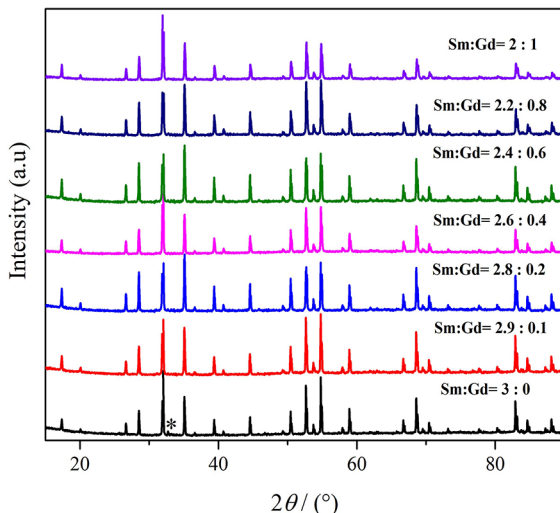


Figure 1. Diffractograms of garnet-type system $\text{Sm}_{3-x}\text{REE}_x\text{Fe}_5\text{O}_{12}$ (REE=Gd) with $x = 0.0, 0.1, 0.2, 0.4, 0.6, 0.8$ and 1.0 . (* SmFeO_3).

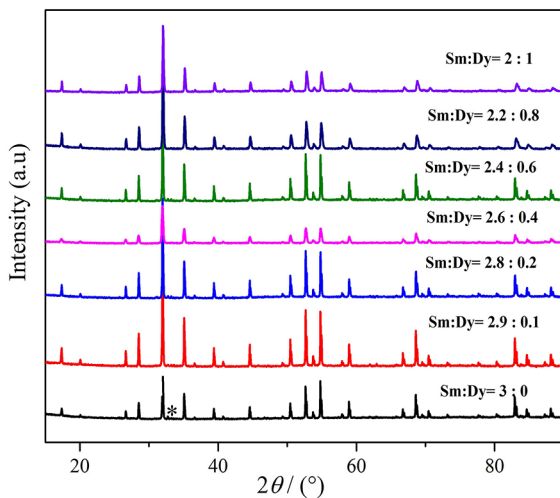


Figure 2. Diffractograms of garnet-type system $\text{Sm}_{3-x}\text{REE}_x\text{Fe}_5\text{O}_{12}$ (REE=Dy) with $x = 0.0, 0.1, 0.2, 0.4, 0.6, 0.8$ and 1.0 . (* SmFeO_3).

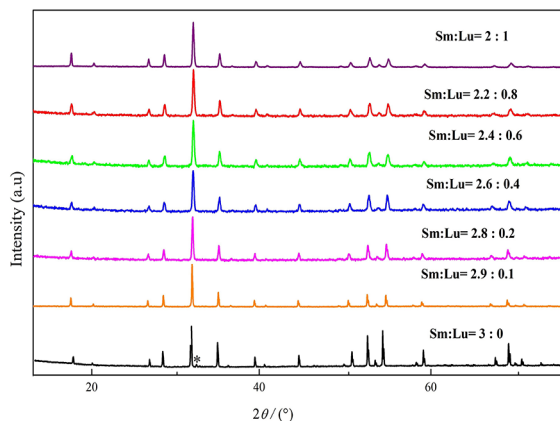


Figure 3. Diffractograms of garnet-type system $\text{Sm}_{3-x}\text{REE}_x\text{Fe}_5\text{O}_{12}$ (REE=Lu) with $x = 0.0, 0.1, 0.2, 0.4, 0.6, 0.8$ and 1.0 . (* SmFeO_3).

Fig. 4 shows the high correlation of the experimental pattern with the theoretical one reported ($\text{Sm}_3\text{Fe}_5\text{O}_{12}$), with the presence of a signal located at 32.8° 2 Theta, which corresponds samarium orthoferrite phase (SmFeO_3), obtained at temperatures between 700°C and 850°C , it is characterized by an antiferromagnetic behavior that negatively influences the magnetic properties of the garnet¹⁷.

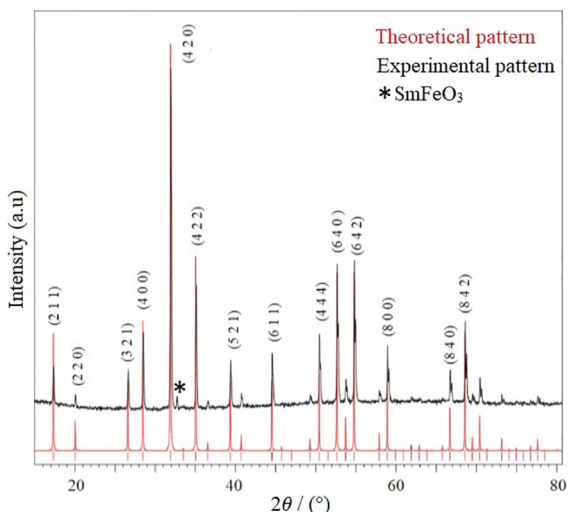


Figure 4. Diffractiongram of theoretical and experimental from $\text{Sm}_3\text{Fe}_5\text{O}_{12}$.

The detailed XRD analysis showed a shift of the patterns to higher angles as the degree of substitution of the rare earths increases. Fig. 5 (a) shows the enlarged region of the main signal for the diffractogram of the $\text{Sm}_{3-x}\text{REE}_x\text{Fe}_5\text{O}_{12}$ system with $x = 0.0, 0.8$ and 1.0 for Gd, Dy and Lu, corresponding to the orientation in the plane (4 2 0). The similarity in each one of the signals obtained and the observed shift, reveal the contraction of the unit cell, which is attributed to the correct substitution at the dodecahedral site for each of the rare earth cations (Fig.5 (b)), at the same time related to the change in crystal size, as was been demonstrated by Muttashar *et al.*¹⁸ and Wu *et al.*¹⁹.

Crystal sizes are shown in Table 1, they were calculated using the Scherrer equation, replacing the values of the strongest signal with a constant of 0.9, where values between 70 and 36 nm were obtained. The smallest values were related to the system substituted with lutetium (Lu). The crystal size decreases with the percentage of substitution of samarium; these properties are explained as a function of the ionic radius of substituted rare earth¹³. The ionic radii are 1.04 \AA for the Sm^{3+} , 1.02 \AA for the Gd^{3+} , 0.99 \AA for the Dy^{3+} and 0.93 \AA for the Lu^{3+} ; the difference of 10.6% in the ionic radius of the smallest cation (Lu) with the main cation favors the cohesion of the unit cell when it is substituted on the dodecahedral site of the structure, which results in lower lattice parameters¹⁵.

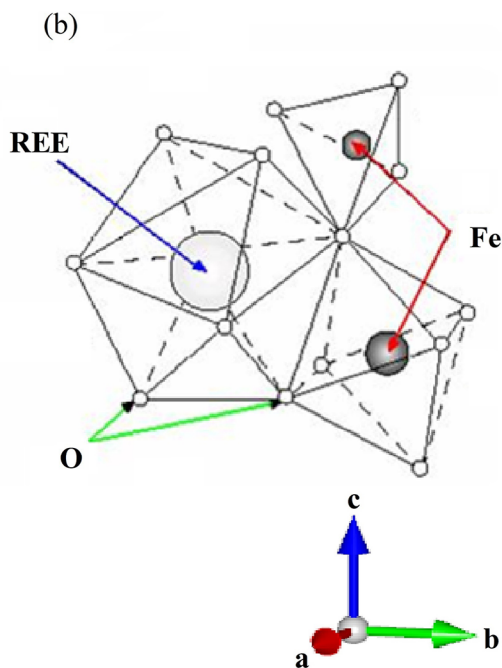
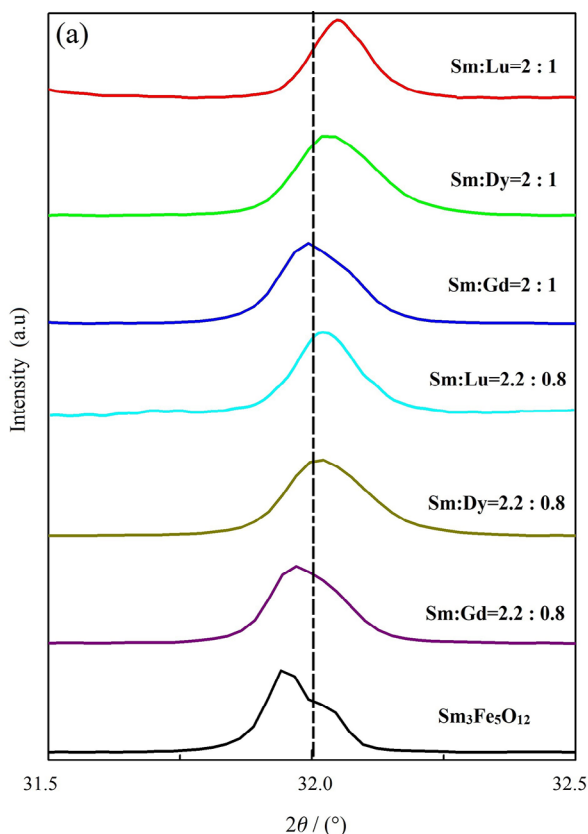


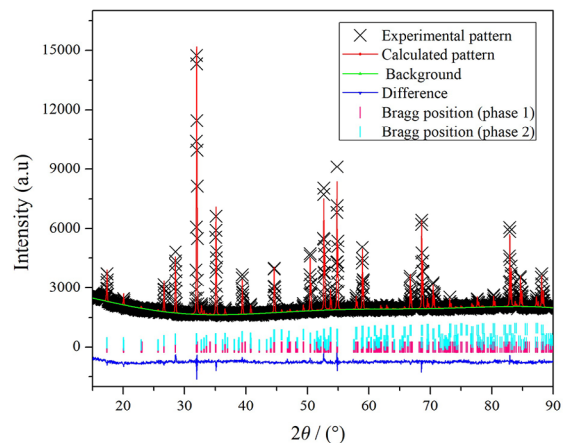
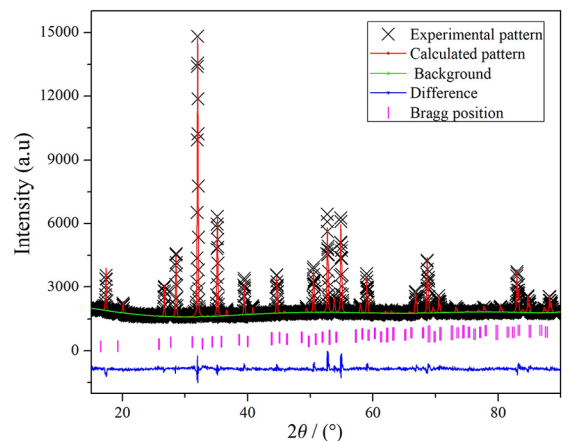
Figure 5. (a) Enlarged region of the main signal from the $\text{Sm}_{3-x}\text{REE}_x\text{Fe}_5\text{O}_{12}$ system (REE= Gd, Dy and Lu) with $x = 0.0, 0.8$ and 1.0 , (b) local polyhedral adopted by the Fe^{3+} and RE^{3+} ion.

Table 1. Rietveld refinement results obtained from the XRD patterns of the garnet-type $\text{Sm}_{3-x}\text{REE}_x\text{Fe}_5\text{O}_{12}$.

REE	X Value	X ²	R(%)	a=b=c (Å)	U _{iso}	Crystallite size (nm)	Link angle Fe(a)-O-Fe(d)	Particle size μm
Gd	0.0	1.61	8.85	12.53(7)	0.025	70	128.89(7)	1.35(4)
	0.1	1.60	11.89	12.55(1)	0.025	61	128.17(4)	3.20(8)
	0.2	1.84	16.69	12.52(8)	0.025	65	128.56(9)	3.43(4)
	0.4	1.84	16.15	12.53(2)	0.025	56	125.76(9)	3.61(1)
	0.6	1.01	9.21	12.51(3)	0.025	58	128.44(2)	3.33(6)
	0.8	2.65	13.07	12.52(8)	0.025	58	128.84(2)	3.21(8)
	1.0	1.89	11.82	12.49(4)	0.025	56	129.71(2)	3.26(8)
Dy	0.1	2.86	10.54	12.53(6)	0.025	66	129.03(5)	2.89(7)
	0.2	2.74	14.16	12.52(5)	0.025	67	129.03(5)	3.08(5)
	0.4	1.52	16.62	12.52(9)	0.025	36	130.42(9)	2.53(7)
	0.6	1.01	10.17	12.49(2)	0.025	53	132.94(0)	2.38(7)
	0.8	1.75	8.57	12.49(7)	0.025	51	128.56(1)	2.21(8)
	1.0	1.12	9.71	12.49(5)	0.025	51	125.77(8)	2.01(6)
Lu	0.1	1.83	16.29	12.51(7)	0.025	66	131.27(1)	3.57(9)
	0.2	1.26	13.08	12.51(1)	0.025	42	131.67(6)	3.65(2)
	0.4	1.24	9.30	12.49(4)	0.025	36	129.00(1)	3.04(4)
	0.6	1.31	14.81	12.48(5)	0.025	36	128.85(8)	2.53(3)
	0.8	1.44	13.56	12.46(9)	0.025	40	127.90(1)	3.02(4)
	1.0	1.17	9.95	12.45(1)	0.025	44	125.65(9)	2.28(1)

The analyses by X-ray diffraction results in tablets were carried out through the Rietveld refinement method using the GSAS and PCW software; Figs. 6 to 9 show the diffractograms refined for $x = 0.0$ and 1.0 of $\text{Sm}_{3-x}\text{REE}_x\text{Fe}_5\text{O}_{12}$ (REE = Gd, Dy and Lu). The refinement performed for the sample with $x = 0$ ($\text{Sm}_3\text{Fe}_5\text{O}_{12}$) showed the presence of a secondary phase of SmFeO_3 that corresponded to 5.4%, with orthorhombic crystalline structure of space group $Pbnm$ (62) with lattice parameters $a = 5.40$ (5) Å, $b = 5.59$ (4) Å and $c = 7.71$ (4) Å and cell volume of 233.29 Å³. The analyses of all the samples confirmed that the substitution with elements such as Gd, Dy and Lu in any of the established values of x , favor the stability of the crystalline phase desired and the obtaining of pure phase, which is corroborated by the small values of refinement parameters (R (%)) and X²) obtained and shown in Table 1, which indicate that the samples synthesized adopt the garnet-type structure.

Rietveld refinement results and the absence of secondary phases confirm that this synthesis process was optimal to favor the ions interdiffusion and the precursors reaction²⁰, using a temperature 200 °C lower than reported by other authors. The insertion of rare earth elements favors crystalline-phase stability and allows to be obtained at lower temperature than reported. By the solid state reaction method, Liu *et al.* in 2017 synthesized iron-samarium garnet ($\text{Sm}_3\text{Fe}_5\text{O}_{12}$) without secondary phases at a temperature of 1400 °C⁹. Aakansha *et al.* synthesized a similar system of iron garnet-yttrium substituted with samarium ($\text{Y}_{3-x}\text{Sm}_x\text{Fe}_5\text{O}_{12}$ with $x = 0.0, 0.5, 1.0, 2.0$ and 3.0) of pure phase, by the method of reaction of solid state, in medium of acetone and with a sintering temperature of 1400 °C⁸.

**Figure 6.** Rietveld refinement results for sample $\text{Sm}_3\text{Fe}_5\text{O}_{12}$.**Figure 7.** Rietveld refinement results for sample $\text{Sm}_2\text{GdFe}_5\text{O}_{12}$.

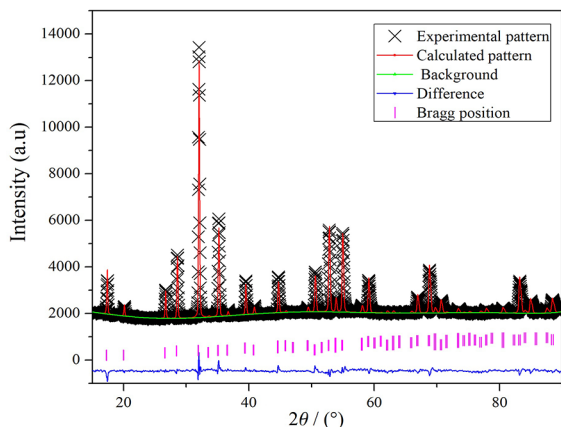


Figure 8. Rietveld refinement results for sample $\text{Sm}_2\text{DyFe}_5\text{O}_{12}$.

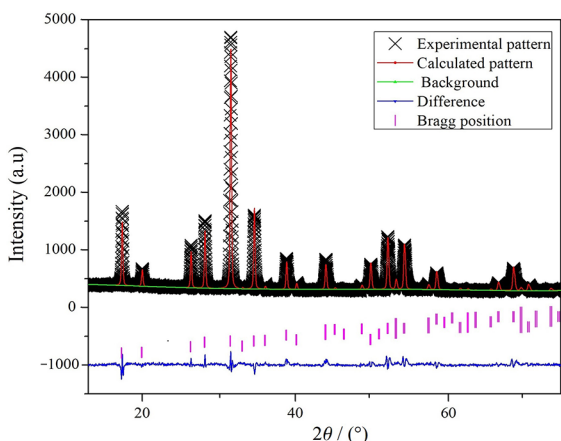


Figure 9. Rietveld refinement results for sample $\text{Sm}_2\text{LuFe}_5\text{O}_{12}$.

The synthesis method used in comparison to chemical methods, does not generate polluting gases or any type of by-product, due to it does not require the use of solvents. Also, the method allows to obtain materials with higher crystallinity.

From the results obtained by Rietveld refinement, it was determined that as the concentrations of Gd^{3+} , Dy^{3+} and Lu^{3+} ions increase, the binding angle of $\text{Fe(a)}-\text{O}-\text{Fe(d)}$ is modified (Table 1), indicating that the distortion of local polyhedral causes a modification in the lattice parameters. Fig. 10 (a) shows the trends of the lattice parameters obtained from the Rietveld refinement for each one of the systems synthesized; the inclusion of rare earth elements with smaller ionic radius causes a modification in the local polyhedral (Fig. 10) (b)), which is represented by smaller lattice parameters ²¹.

In order to verify different distortions of the local polyhedral, Raman spectroscopy was performed, in which the cubic symmetry presents $3A_{1g} + 8E_g + T_{2g}$ as active translational and rotational modes²². The spectra are shown in Fig.11 - 13; these results are characteristic of garnet-type materials, which indicate that the Gd^{3+} , Dy^{3+} and Lu^{3+} ions were properly integrated in the structure. The signals located on 150 cm^{-1} , 250 cm^{-1} and 325 cm^{-1} are attributed to vibrational modes of Sm^{3+} and other REE^{3+} in the dodecahedron and vibrational modes of $\text{Fe}-\text{O}$ in the tetrahedron and octahedron²³, all this is in concordance with what was previously reported by Wu *et al.*¹⁹; in addition, the signals located from 350 to 800 cm^{-1} are result from stretching and reflection of the tetrahedron (FeO_4)²⁴. Fig. 14 shows the enlarged main signal from Raman spectra of the system samples ($\text{Sm}_{3-x}\text{REE}_x\text{Fe}_5\text{O}_{12}$ (REE = Gd, Dy and Lu) with $x = 0.0$ and 1.0), where the shift of the signals at different frequencies depending on the element of substituent earth, which is attributed to the modification of bond lengths and angles between atoms, it occurs thanks to the rare earth substitution¹⁹.

The analysis by Rietveld refinement allowed to calculate the $\text{Fe(d)}-\text{O}$ bond distance of 1.89 \AA for $\text{Sm}_2\text{DyFe}_5\text{O}_{12}$, 1.88 \AA for $\text{Sm}_2\text{LuFe}_5\text{O}_{12}$, 1.84 \AA for $\text{Sm}_2\text{GdFe}_5\text{O}_{12}$ and 1.81 \AA for $\text{Sm}_3\text{Fe}_5\text{O}_{12}$.

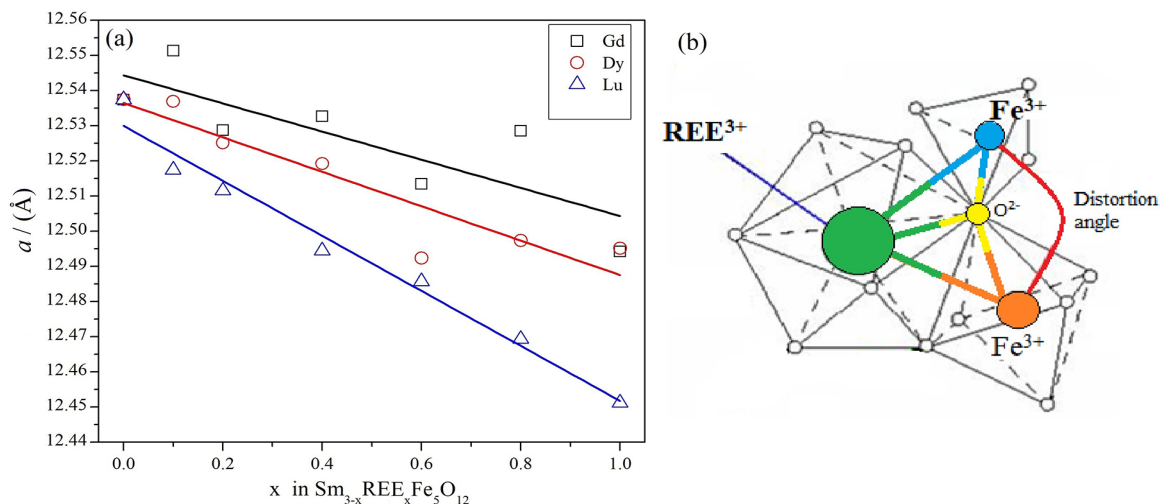


Figure 10. (a) Lattice parameter vs x value for garnet-system $\text{Sm}_{3-x}\text{REE}_x\text{Fe}_5\text{O}_{12}$ (REE= Gd, Dy y Lu) and (b) distortion angle experienced by local polyhedral.

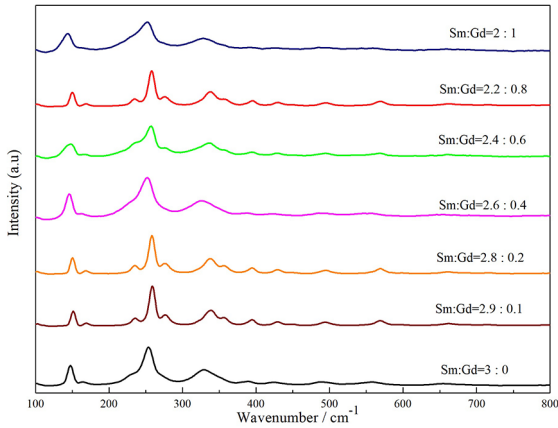


Figure 11. Raman spectra of garnet-system $\text{Sm}_{3-x}\text{Gd}_x\text{Fe}_5\text{O}_{12}$ with $x = 0.0, 0.1, 0.2, 0.4, 0.6, 0.8$ and 1.0 .

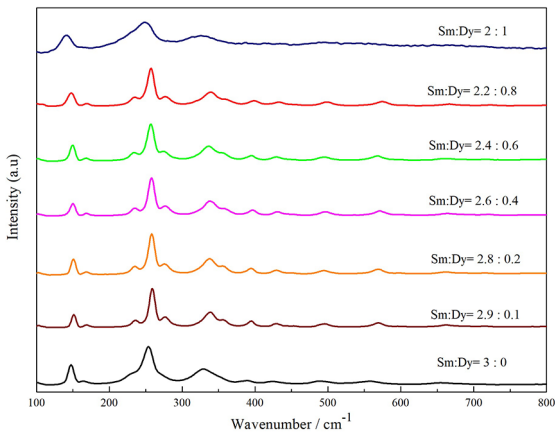


Figure 12. Raman spectra of garnet-system $\text{Sm}_{3-x}\text{Dy}_x\text{Fe}_5\text{O}_{12}$ with $x = 0.0, 0.1, 0.2, 0.4, 0.6, 0.8$ and 1.0 .

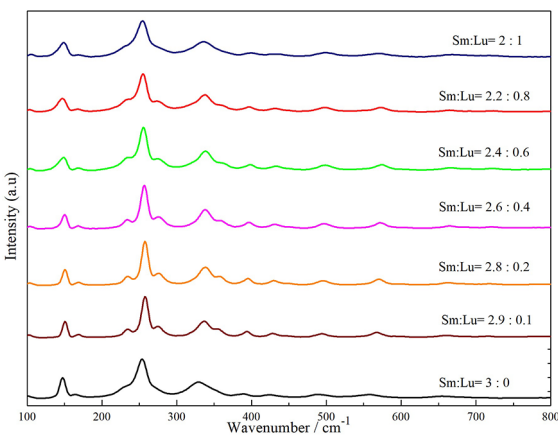


Figure 13. Raman spectra of garnet-system $\text{Sm}_{3-x}\text{Lu}_x\text{Fe}_5\text{O}_{12}$ with $x = 0.0, 0.1, 0.2, 0.4, 0.6, 0.8$ and 1.0 .

These values explain why the Raman spectrum of $\text{Sm}_3\text{Fe}_5\text{O}_{12}$ is located at higher wave numbers and that of $\text{Sm}_2\text{DyFe}_5\text{O}_{12}$ is displaced to lower wave numbers; this is attributed to

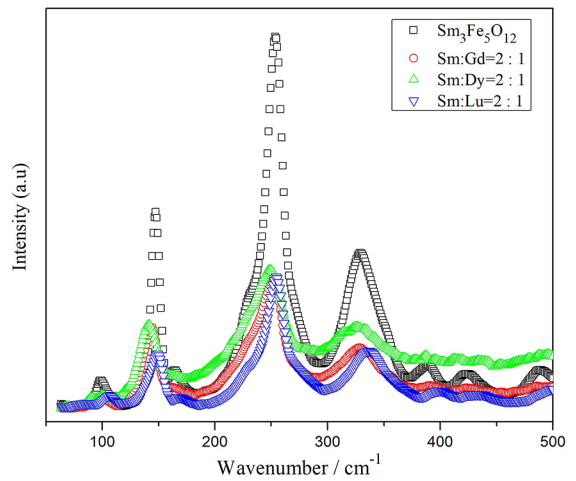


Figure 14. Amplified region Raman spectrum of the garnet-system $\text{Sm}_{3-x}\text{RE}_x\text{Fe}_5\text{O}_{12}$ (RE = Gd, Dy and Lu) with $x = 0.0$ and 1.0 .

the fact that for a harmonic oscillator, the frequency of vibration is proportional to the square root of the binding force²², the frequency is affected by the angular distribution of the adjacent oxygens. The increasing in the size of substituent cation causes repulsion effects what generates the tetrahedron contraction, this demonstrates that the substitution by elements of rare earths in the garnets has been performed in an accurate way, modifying the bond distances and angles between atoms but not the type of crystal structure^{24,25}.

3.2 Morphological analysis

The Fig. 15 show the micrographs obtained with secondary electrons for the garnets $\text{Sm}_{3-x}\text{RE}_x\text{Fe}_5\text{O}_{12}$ (RE =Gd, Dy and Lu with $x = 0.0$ and 1.0), the formation of particles with well-defined edges are observed, these characteristics are due to sintering process and the rare earth substituted which modify the arrangement of the particles. When samarium is substituted by gadolinium, the particle size is greater (Fig. 15 b), the characteristics of these particles depend on the nucleation process and growth rate, which can be highly influenced by the substitution with REE, affecting their alignment sizes and shapes²⁶.

Using the Image J software, the particle size was determined using image taken at 10000x, the average particle size was determined for each of the synthesized garnets. Table 1 shows the particle size values obtained, the larger particles are associated with the substitution with the Gd^{3+} ion, which is in accordance with the larger crystal size obtained by XRD, the substitution of Sm^{3+} promotes the formation of larger particles²⁷, this is in accordance with the results obtained by Liu *et al.* who studied the dependence of optical and thermochromic properties respect particle size of $\text{Sm}_3\text{Fe}_5\text{O}_{12}$ ⁹.

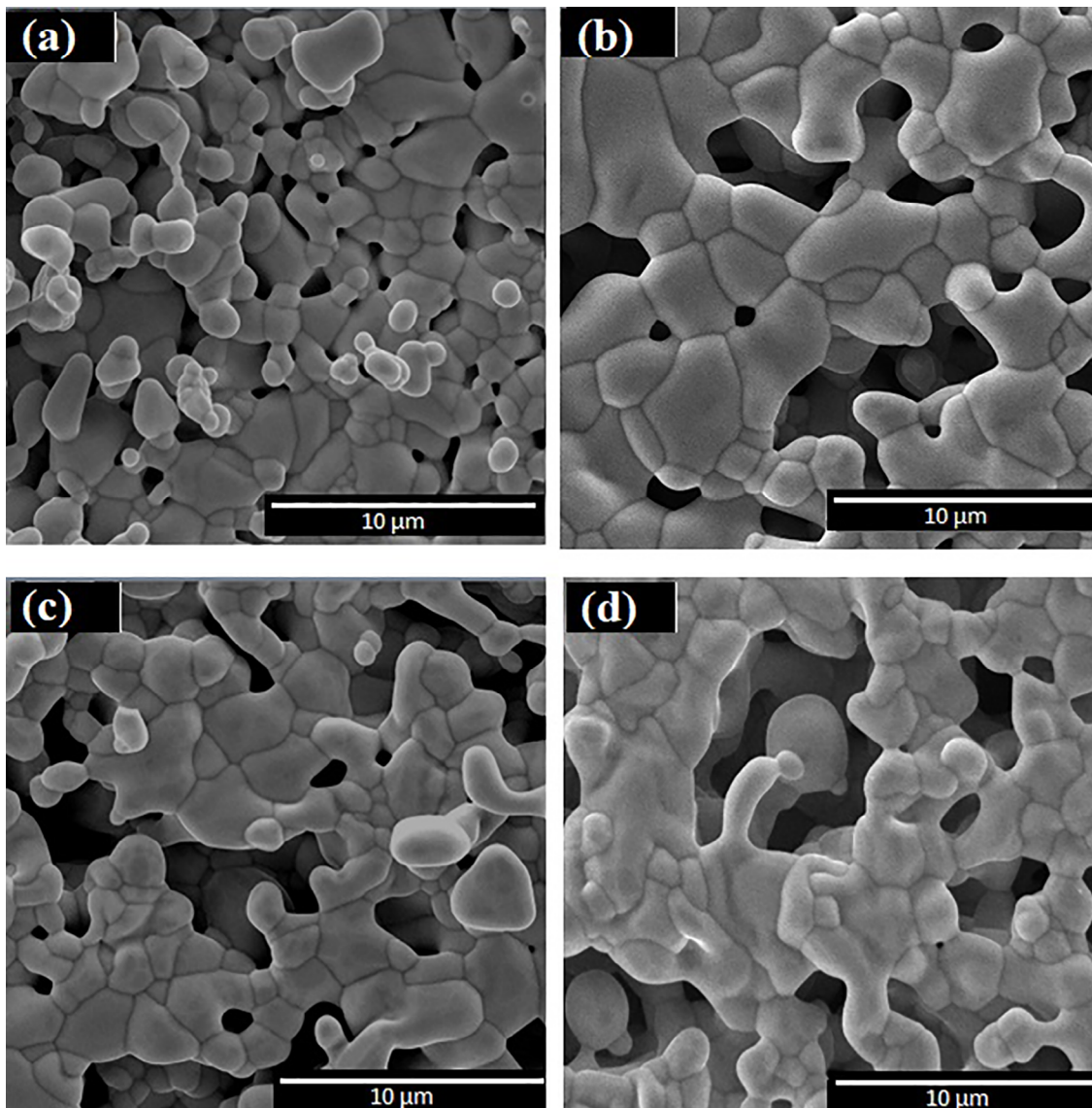


Figure 15. Micrographs of $\text{Sm}_{3-x}\text{REE}_x\text{Fe}_5\text{O}_{12}$ (REE = Gd, Dy and Lu) with $x = 0.0$ and 1.0 .

4. Conclusion

New garnets $\text{Sm}_{3-x}\text{REE}_x\text{Fe}_5\text{O}_{12}$ (REE = Gd, Dy and Lu, $x = 0.0 - 1.0$) were synthesized by the solid-state reaction method at lower temperature than previously reported by other authors. The Rietveld refinement showed the presence of 5.4% of SmFeO_3 phase in the garnet ($\text{Sm}_3\text{Fe}_5\text{O}_{12}$). The substitution with rare earth cations in dodecahedral site favors the stability of single phase with cubic structure and space group $Ia\bar{3}d$ (230), and crystal size between 36 and 70 nm, the smallest values were related to Lu^{3+} cation, which is explained according to the ionic radius for the structural cohesion. The characterization confirmed that the rare earth ions substituents were integrated into the garnet structure. The samarium substitution caused a modification of angles and bond lengths in the garnet structure and an increase in the particle sizes.

5. Acknowledgement

We would like to thank at the Administrative. Department of Science, Technology and Innovation from Colombia (Colciencias) for the financing of this work.

6. References

1. Nakamoto R, Xu B, Xu C, Xu H, Bellaiche L. Properties of rare-earth iron garnets from first principles. *Physical Review B*. 2017;95(2):024434.
2. Wang J, Yang J, Jin Y, Qiu T. Effect of manganese addition on the microstructure and electromagnetic properties of YIG. *Journal of Rare Earths*. 2011;29(6):562-566.
3. Gavriluk AG, Struzhkin VV, Lyubutin IS, Eremets MI, Trojan IA, Artemov VV. Equation of state and high-pressure irreversible amorphization in $\text{Y}_3\text{Fe}_5\text{O}_{12}$ composition. *JETP Letters*. 2006;83(1):37-41.

4. Guo X, Tavakoli AH, Sutton S, Kukkadapu RK, Qi L, Lanzirotti A, et al. Cerium substitution in yttrium iron garnet: valence state, structure, and energetics. *Chemistry of Materials*. 2013;26(2):1133-1143.
5. Ibrahim NBY, Arsad A. Investigation of nanostructural, optical and magnetic properties of cerium-substituted yttrium iron garnet films prepared by a sol gel method. *Journal of Magnetism and Magnetic Materials*. 2016;401:572-578.
6. Huang S, Shi LR, Sun HG, Li CL, Chen L, Yuan SL. High temperature dielectric response in $\text{Sm}_3\text{Fe}_5\text{O}_{12}$ ceramics. *Journal of Alloys and Compounds*. 2016;674:341-346.
7. Hernández-Gómez P, Torres C, Francisco C, Iñiguez JI, Perdigo JM. Analysis of phase transitions in Ia and Nd substituted YIG with magnetic disaccommodation measurement. *Materials Science Forum. Trans Tech Publ*. 2006;514-516:319-322.
8. Aakansha, Deka B, Ravi S, Pamu D. Impedance spectroscopy and ac conductivity mechanism in Sm doped yttrium iron garnet. *Ceramics International*. 2017;43(13):10468-10477.
9. Liu H, Yuan L, Qi H, Du Y, Wang S, Hou C. Size-dependent optical and thermochromic properties of $\text{Sm}_3\text{Fe}_5\text{O}_{12}$. *RSC Advances*. 2017;7(60):37765-37770.
10. Jang MS, Roh IJ, Park J, Kang CY, Choi WJ, Baek SH, et al. Dramatic enhancement of the saturation magnetization of a sol-gel synthesized $\text{Y}_3\text{Fe}_5\text{O}_{12}$ by a mechanical pressing process. *Journal of Alloys and Compounds*. 2017;711:693-697.
11. Tholkappiyan R, Vishista K. Tuning the composition and magnetostructure of dysprosium iron garnets by Co-substitution: An XRD, FT-IR, XPS and VSM study. *Applied Surface Science*. 2015;351:1016-1024.
12. Ramesh T, Shinde RS, Murthy SR. Nanocrystalline gadolinium iron garnet for circulator applications. *Journal of Magnetism and Magnetic Materials*. 2012;324(22):3668-3673.
13. Patel SKS, Lee JH, Bhoi B, Lim JT, Kim CS, Kim SK. Effects of isovalent substitution on structural and magnetic properties of nanocrystalline $\text{Y}_{3-x}\text{Gd}_x\text{Fe}_5\text{O}_{12}$ ($0 \leq x \leq 3$) garnets. *Journal of Magnetism and Magnetic Materials*. 2018;452:48-54.
14. Praveena K, Srinath S. Effect of Gd^{3+} on dielectric and magnetic properties of $\text{Y}_3\text{Fe}_5\text{O}_{12}$. *Journal of Magnetism and Magnetic Materials*. 2014;349:45-50.
15. Cheng Z, Yang H. Synthesis and magnetic properties of $\text{Sm-Y}_3\text{Fe}_5\text{O}_{12}$ nanoparticles. *Physica E: Low-dimensional Systems and Nanostructure*. 2007;39(2):198-202.
16. Kumar KA, Manimuthu P, Ezhilarasi VS, Venkateswaran C. Grain size dependent magneto-dielectric studies on $\text{Lu}_3\text{Fe}_5\text{O}_{12}$. *Physica B: Condensed Matter*. 2014;448:333-335.
17. Sattar AA, Elsayed HM, Faramawy AM. Comparative study of structure and magnetic properties of micro- and nano-sized $\text{Gd}_x\text{Y}_{3-x}\text{Fe}_5\text{O}_{12}$ garnet. *Journal of Magnetism and Magnetic Materials*. 2016;412:172-180.
18. Muttashar HL, Ali NB, Ariffin MAM, Hussin MW. Microstructures and physical properties of waste garnets as a promising construction materials. *Case Studies in Construction Materials*. 2018;8:87-96.
19. Wu H, Huang F, Xu T, Ti R, Lu X, Kan Y, et al. Magnetic and magnetodielectric properties of $\text{Y}_{3-x}\text{La}_x\text{Fe}_5\text{O}_{12}$ ceramics. *Journal of Applied Physics*. 2015;117(14):144101.
20. Valenzuela R. *Magnetic ceramics*. Cambridge: Cambridge University Press; 2005.
21. Patel SKS, Kurian S, Gajbhiye NS. Room-temperature ferromagnetism of Fe-doped TiO_2 nanoparticles driven by oxygen vacancy. *Materials Research Bulletin*. 2013;48(2):655-660.
22. Sharma V, Kuanr BK. Magnetic and crystallographic properties of rare earth substituted yttrium-iron garnet. *Journal of Alloys and Compounds*. 2018;748:591-600.
23. Wu HR, Ti RX, Xu Y, Shan YZ. Dielectric property of $\text{Y}_{2.7}\text{La}_{0.3}\text{Fe}_5\text{O}_{12}$ ceramics. *Physica B: Physics of Condensed Matter*. 2018;530:15-18.
24. Fechine PBA, Silva EN, Menezes AS, Derov J, Stewart JW, Drehman AJ, et al. Synthesis, structure and vibrational properties of $\text{GdIG}_x\text{:YIG}_{1-x}$ ferrimagnetic ceramic composite. *Journal of Physics and Chemistry of Solids*. 2009;70(1):202-209.
25. Siao YJ, Qi XD. Dielectric responses in polycrystalline rare-earth iron garnets. *Journal of Alloys and Compounds*. 2017;691:672-682.
26. Kang SJ. *Sintering: densification, grain growth and microstructure*. Oxford: Butterworth-Heinemann; 2004.
27. Akhtar MN, Yousaf M, Khan SN, Nazir MS, Ahmad M, Khan MA. Structural and electromagnetic evaluations of YIG rare earth doped (Gd, Pr, Ho, Yb) nanoferrites for high frequency applications. *Ceramics International*. 2017;43(18):17032-17040.